FEBS Letters 580 (2006) 1681–1684

Kinetics of amyloid aggregation of mammal apomyoglobins and correlation with their amino acid sequences

Silvia Vilasi[a,c], Roberta Dosi[b], Clara Iannuzzi[a], Clorinda Malmo[a], Augusto Parente[b], Gaetano Irace[a], Ivana Sirangelo[a,*]

[a] Dipartimento di Biochimica e Biofisica, Seconda Università degli Studi di Napoli, Via L. De Crecchio 7, 80138 Naples, Italy
[b] Dipartimento di Scienze della Vita, Seconda Università degli Studi di Napoli, Via Vivaldi, 81100 Caserta, Italy
[c] Istituto Nazionale di Fisica Nucleare, Sezione di Napoli, GC Salerno, Italy

Received 25 January 2006; accepted 6 February 2006

Available online 17 February 2006

Edited by Judit Ovádi

Abstract In protein deposition disorders, a normally soluble protein is deposited as insoluble aggregates, referred to as amyloid. The intrinsic effects of specific mutations on the rates of protein aggregation and amyloid formation of unfolded polypeptide chains can be correlated with changes in hydrophobicity, propensity to convert α-helical to β sheet conformation and charge. In this paper, we report the aggregation rates of buffalo, horse and bovine apomyoglobins. The experimental values were compared with the theoretical ones evaluated considering the amino acid differences among the sequences. Our results show that the mutations which play critical roles in the rate-determining step of apomyoglobin aggregation are those located within the N-terminal region of the molecule.

Keywords: Protein aggregation rate; Apomyoglobin aggregation; Amyloid

1. Introduction

A large family of human diseases is characterized by the presence, in tissues, of highly ordered insoluble protein aggregates known as amyloid fibrils [1]. The aggregation process is generally believed to initiate from partially folded or completely unfolded states of proteins normally present in tissues in soluble form [2]. The events leading to the transformation of a soluble protein into insoluble amyloid fibrils consist of a conformational change which exposes part of the main-chain and hydrophobic residues to the solvent under conditions in which intermolecular interactions can take place. This process leads to the formation of species competent for self-association which assemble into amyloid fibrils following a nucleation–polymerization mechanism [3].

Microscopic and X-ray techniques indicate that the morphology of fibrillar aggregates shares common features even if the proteins involved differ in their sequence and native structure. Fibrils are straight and unbranched, 5–10 nm wide, and characterized by β-strands oriented perpendicularly to the long axis of the fibril [4–8].

Moreover, proteins which are not involved in any disease are also able to form amyloid fibrils which are morphologically and structurally indistinguishable from those formed by pathological proteins [9–14]. Therefore, the ability to form amyloid could be a generic property of proteins closely linked to main-chain interactions [15–17]. However, the extent and rate of fibril formation are related to side-chain properties [18,19].

The propensity of a given protein to aggregate and form amyloid fibrils under specific conditions depends dramatically on its amino acid sequence. Some human genetic amyloid diseases are caused by point mutations [20–22]. The mechanism by which a mutation increases the aggregation propensity has not yet been understood perfectly. It is believed that some mutations destabilize the native state favoring the formation of partially folded states which are more prone to aggregation. This is because hydrophobic residues, which are largely buried within the core of the native protein, become more exposed [3]. Nevertheless, in some amyloidoses, the aggregation involves direct self-assembly of unstructured protein conformations [23].

It has been shown that intrinsic effects of specific mutations on the rate of aggregation of unfolded polypeptide chains can be related to changes of physicochemical properties such as hydrophobicity (ΔHy), propensity to convert from α-helical to β-sheet ($\Delta\Delta G_{\alpha\text{-coil}} + \Delta\Delta G_{\text{coil-}\beta}$) and overall charge ($\Delta Q$) [24]. The variation in aggregation rate caused by a mutation is related to the contributions of these three independent and additive factors by the relationship:

$$\ln\left(\frac{v_{\text{mut}}}{v_{\text{wt}}}\right) = A\Delta\text{Hy} + B(\Delta\Delta G_{\alpha\text{-coil}} + \Delta\Delta G_{\text{coil-}\beta}) + C\Delta Q, \qquad (1)$$

where $A = 0.633$, $B = 0.198$ and $C = -0.491$ [24]. The negative C value results from the fact that the effect of net charge on protein aggregation and amyloidogenicity is in opposition to the other two factors [25].

The aim of this study is to relate the variations in the amyloid aggregation rates of mammal apomyoglobins to the differences in amino acid sequence. Even apomyoglobin, a globular protein which contains only α-helical structures, forms amyloid fibrils due to association of unfolded polypeptide segments if incubated at 65 °C and at pH 9.0 [12,26]. The aggregation rates of buffalo, horse and bovine apomyoglobins were measured. These proteins can be considered natural mutants because

*Corresponding author. Fax: +39 81 5665863.
E-mail address: Ivana.Sirangelo@unina2.it (I. Sirangelo).

Abbreviations: ThT, Thioflavin T; Mb, myoglobin

0014-5793/$32.00
doi:10.1016/j.febslet.2006.02.018

their amino acid sequence differs in a few residues. The differences observed were compared to the theoretical ones calculated by using Eq. (1). The results demonstrate that the variations in amyloid aggregation kinetics are related only to the amino acid differences in the N-terminal region of the proteins. This suggests that the N-terminal region is involved in the rate-determining step of apomyoglobin aggregation.

2. Materials and methods

2.1. Apomyoglobins

Buffalo and bovine myoglobins (Mbs) were purified from *longissimus dorsi* essentially using the procedure reported by Balestrieri et al. [27] with some modifications.

Frozen muscle was thawed overnight at 4 °C, partially freed of gross fat and connective tissue, cut into small pieces, that were placed in Milli Q water (1:1; w:v) and homogenated in a Waring Blender homogenizer. The homogenate was then centrifuged at 14000 rpm for 40 min at 4 °C, and the supernatant was filtered through Mirachlot paper (Calbiochem, San Diego – USA) to remove fatty material. The clear filtrate was then dialyzed, using a Spectra/Por® membrane (molecular mass cut off 6000–8000) against Milli Q water. The white precipitate formed during the dialysis was removed by centrifugation at 14000 rpm for 15 min. 20 mL of the supernatant (protein concentration about 10 mg/mL) were gel-filtered onto a S-Sephacryl column (ϕ 2.6 × 115 cm, Amersham Pharmacia Biotech, Milano – Italy), equilibrated with 25 mM NaH_2PO_4–0.35 M NaCl buffer, pH 7.2. The column was then eluted with the same buffer at a flow rate of 35 mL/h, collecting 5 mL fractions. The eluate was monitored at 280 and 409 nm.

The Mb-containing fractions were concentrated on an ultrafiltration cell (Amicon Inc., Beverly, USA), using a membrane with molecular mass cut-off 10000, and then dialyzed against 10 mM Tris · Cl, pH 8.6 (Buffer A). The dialyzed protein solution was centrifuged at 14000 rpm for 15 min, at 4 °C. The supernatant was absorbed onto a DEAE–Sepharose column (ϕ 3 × 8 cm, BioRad, Milano, Italy), equilibrated with Buffer A and eluted with a gradient made up by Buffer A and Buffer B (10 mM Tris · Cl, pH 8.6 containing 0.5 M NaCl), at a flow rate of 1.5 mL/min. The eluate absorbance was measured at 280 and 409 nm and the sample purity checked by SDS–PAGE.

Horse Mb from skeletal muscle was obtained from Sigma.

The heme was removed from Mbs by the 2-butanone extraction procedure [28]. Protein concentrations were determined measuring absorption (Jasco V-550 spectrophotometer) at 280 nm using 13500 M^{-1} cm^{-1} as molar extinction coefficient [29].

2.2. Aggregation kinetics

Apomyoglobin fibrils were obtained incubating 40 μM of protein in 50 mM sodium borate, pH 9.0 at 65 °C [12]. Aggregation was monitored by Thioflavin T (ThT) fluorescence and far UV CD at 216 nm. Fibril formation was confirmed by AFM images.

Aliquots of proteins were taken at different times and mixed with 25 μM of ThT. The molar ratio protein/ThT was 2:5. ThT fluorescence was determined by a Perkin–Elmer Life Sciences LS 55 spectrofluorimeter at the excitation and emission wavelengths of 450 and 482 nm, respectively. The fluorescence intensity at 482 nm was corrected by subtracting the emission intensity recorded before the addition of protein to thioflavin T solutions.

Far UV CD measurements were performed on a Jasco J-715 spectropolarimeter using thermostated quartz cells of 0.1 cm path length.

Fluorescence intensity was plotted as function of time and interpolated to single exponential function as

$$y = y_0 + Ke^{-\frac{t}{\tau}}, \quad (2)$$

where τ is the inverse of aggregation rate (v), y_0 is the maximal signal intensity corresponding to the maximal aggregation and K the difference between the maximal and the initial signal intensity. Differences in the protein aggregation rate were expressed as $\ln(v/v_{ref})_{exp}$, where v is the aggregation rate of the given protein and v_{ref} is that of the reference protein [19].

3. Results and discussion

In this paper, we compare the aggregation rates of buffalo and horse apomyoglobins with that of bovine apomyoglobin which we used as a reference protein. Aggregation rates were determined following the time dependence of ThT fluorescence and CD ellipticity at 216 nm upon incubation of proteins at pH 9.0 and 65 °C. In these conditions, apomyoglobin is destabilized and forms fibrillar aggregates as indicated by electron microscopy [12,26]. ThT is a fluorescent dye which is known to detect reliably the formation of amyloid fibrils due to the significant increase in its emission intensity upon binding to the linear array of β-strands [30]. The aggregation kinetics was also probed by Congo Red absorption (data not shown). The kinetic traces were highly reproducible, and the rates determined using the three techniques were closely correlated.

Fig. 1 shows the aggregation kinetics of the three examined proteins monitored by ThT fluorescence intensity at 482 nm and far UV CD at 216 nm. The aggregation kinetics show an exponential growth phase, characteristic of nucleation-dependent polymerization [15]. A lag phase was not evident probably because of the temperature-induced increase of aggregation rate. The data were fitted to single exponential functions (Eq. (2)). The fit parameters and the corresponding reduced chi-square, χ^2, are reported in Table 1. The aggregation rates (v) of buffalo and horse apomyoglobins were found significantly greater than that of bovine apomyoglobin. The differences in aggregation kinetics were evaluated as $\ln(v/v_{ref})_{exp}$ using bovine apomyoglobin as a reference. The amino acid sequences of the three examined proteins are shown in Fig. 2. For each substitution, we calculated the changes of charge (ΔQ), hydrophobicity (ΔHy) and beta propensity ($\Delta\Delta G_{\alpha\text{-coil}} + \Delta\Delta G_{\text{coil-}\beta}$) (Table 2) using the values reported in the literature [24]. Using Eq. (1), we obtained the theoretical value $\ln(v/v_{ref})_i$ for the ith mutation (starting from N-terminus):

$$\ln\left(\frac{v}{v_{ref}}\right)_i = A\Delta\mathrm{Hy}_i + B(\Delta\Delta G_{\alpha\text{-coil}} + \Delta\Delta G_{\text{coil-}\beta})_i + C\Delta Q_i.$$

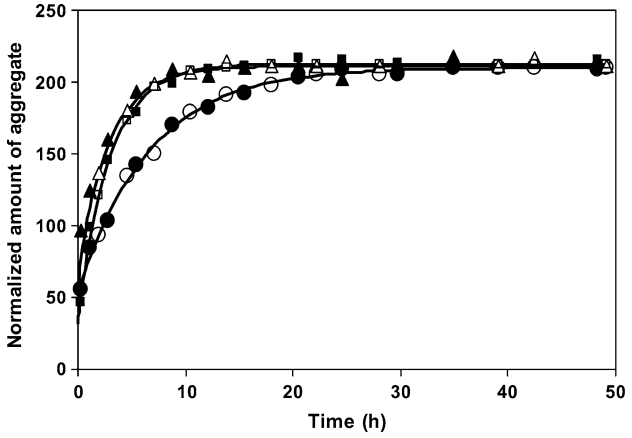

Fig. 1. Time dependence of ThT fluorescence (filled black symbols) and far UV CD at 216 nm (open black symbols) of buffalo (square), bovine (circles) and horse (triangles) apomyoglobins. The continuous lines through the data are the best fits to single exponential functions. The kinetics measured from both techniques are in close agreement.

Table 1
Best fit parameters of the aggregation kinetics for buffalo, bovine and horse apomyoglobins

	Buffalo	Bovine	Horse
K	−180 ± 5	−158 ± 4	−154 ± 6
y_0	213 ± 3	210 ± 2	209 ± 2
τ (h)	2.9 ± 0.6	7 ± 2	2.8 ± 0,7
ν (h^{-1})	0.34 ± 0.07	0.14 ± 0.04	0.36 ± 0.09
χ^2	1.1	0.9	1.1

The theoretical differences in the aggregation rate of buffalo and horse apomyoglobins with respect to bovine apomyoglobin were evaluated by the sum of terms $\ln(\nu/\nu_{ref})_i$ corresponding to each mutation:

$$\ln\left(\frac{\nu_{buf}}{\nu_{bov}}\right)_{theor} = \sum_{i=1}^{3} \ln\left(\frac{\nu_{buf}}{\nu_{bov}}\right)_i,$$

$$\ln\left(\frac{\nu_{horse}}{\nu_{bov}}\right)_{theor} = \sum_{i=1}^{18} \ln\left(\frac{\nu_{horse}}{\nu_{bov}}\right)_i.$$

In Table 3, the theoretical differences in the aggregation rate are reported. It is clear that they significantly differ from the experimentally measured values. The discrepancy between experimental and theoretical values suggests that aggregation may not involve the overall polypeptide chain but only some polypeptide segments, in particular those which are more prone to aggregate. It is not known which apomyoglobin segments are involved in the formation of amyloid fibrils. However, peptide fragments corresponding to the N-terminal region or to the G-helix of Mb have been previously shown to form species with extensive β-structure [31,32]. In this respect, our attention was turned to identify the protein regions which determine the observed aggregation rate variations. We found that crucial substitutions are those present in the N-terminal region of the protein. In this region, buffalo apomyoglobin presents only one substitution, A19T, whereas horse apomyoglobin shows three mutations: L9Q, A13V and V21I. Although these substitutions are all relatively conservative, they introduce changes in hydrophobicity and β sheet formation propensity (see Table 2) which increase the aggregation rate. Moreover, many of them are natural mutations associated with familial diseases [24]. The close similarity of horse and buffalo kinetics data (Fig. 1) is well correlated to the amino acid substitutions in the N-terminal region. In fact, the theoretical values, $\ln(\nu/\nu_{ref})_{N\text{-term}}$, calculated from the contributions supplied by these mutations (Table 3) were consistent with the experimental values, the discrepancy being lower than the experimental errors. On the contrary, the calculations relative to the other helical segments did not provide consistent values. In particular, the mutations in the G helix lead to

Table 2
Physicochemical changes relative to amino acid differences of buffalo and horse Mbs with respect to bovine Mb used as a reference[a]

Mutation	Helix	ΔHy	$\Delta\Delta G_{\alpha\text{-coil}} + \Delta\Delta G_{\text{coil-}\beta}$	ΔQ	$\ln(\nu/\nu_{ref})$
Bovine Mb → buffalo Mb					
A19T	B	−1.39	8.42	0	0.80
A117D	G	−4.2	−3.38	1	−3.82
D141E	H	0.9	2.78	0	1.12
Bovine Mb → horse Mb					
L9Q	A	−3.12	3.63	0	−1.26
A13V	A	0.91	7.01	0	1.96
V21I	B	0.52	−0.56	0	0.22
N66T	E	0.91	4.67	0	1.50
T67V	E	2.3	−0.95	0	1.27
V86L	F	0.52	−2.67	0	−0.20
H88P	F	1.63	5.11	0	2.04
E91Q	F	1.61	0.14	−1	1.54
N95T	/	0.91	4.67	0	1.50
V101I	G	0.52	−0.56	0	0.22
A117S	G	−1.63	2.32	0	−0.57
S121G	H	1.24	−4.09	0	−0.03
A129G	H	−0.39	1.50	0	0.05
S132T	H	0.24	3.12	0	0.77
M142I	H	0.86	2.30	0	1.00
Q145K	H	−1.47	−0.08	1	−1.44
V148E	H	−4.21	−3.00	1	−3.75
H152Q	/	−0.66	0.41	0	−0.34

[a]These changes were evaluated using the data reported in reference [24].

Table 3
Experimental and theoretical variations of the aggregation rates of buffalo and horse apomyoglobins with respect to bovine apomyoglobin used as a reference

	$\ln(\nu/\nu_{ref})_{exp}$	$\ln(\nu/\nu_{ref})_{theor}$	$\ln(\nu/\nu_{ref})_{N\text{-term}}$
Bovine → buffalo	0.88 ± 0.09	−1.90	0.80
Bovine → horse	0.91 ± 0.04	4.48	0.92

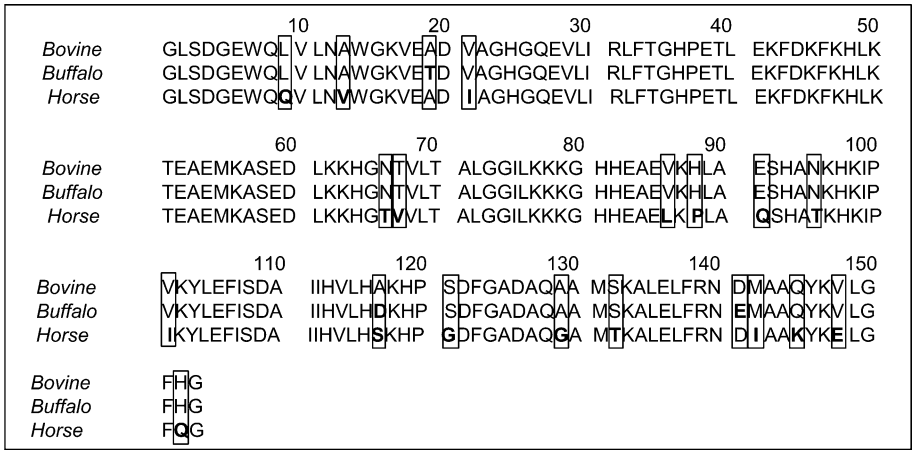

Fig. 2. Comparison of amino acid sequences of buffalo, horse and bovine Mbs. The amino acid differences are highlighted. The amino acid sequence of buffalo Mb was determined by Dosi (unpublished results, see also [33]).

aggregation rates significantly different from the experimental values.

In conclusion, the data reported here suggest that the N-terminal region might form part of the sequence segment that is relevant for the α to β transition of apomyoglobin from a globular state to amyloid fibrils. The observation that the N-terminal region of apomyoglobin is more hydrophobic than the rest of the molecule and, thus, more prone to aggregate [31] further corroborates our conclusion. Moreover, it has been reported that mutations occurring in the A-helix, i.e., W7FW14F, result in the expression of an amyloidogenic apomyoglobin with a high propensity to form amyloid fibrils under physiological conditions [13,14].

Acknowledgments: This work has been supported by a grant from Ministero dell'Università e della Ricerca Scientifica e Tecnologica (FIRB 2003, "Folding e aggregazione di proteine"). Silvia Vilasi thanks "Consorzio Cresci" for partial support.

References

[1] Carrell, R.W. and Lomas, D.A. (1997) Conformational disease. Lancet 350, 134–138.
[2] Stefani, M. and Dobson, C.M. (2003) Protein aggregation and toxicity: new insights into protein folding, misfolding diseases and biological evolution. J. Mol. Med. 81, 678–699.
[3] Kelly, J.W. (1998) The alternative conformations of amyloidogenic proteins and their multi-step assembly pathways. Curr. Opin. Struct. Biol. 8, 101–106.
[4] Serpell, L.C., Sunde, M. and Blake, C.C. (1997) The molecular basis of amyloidosis. Cell. Mol. Life Sci. 53, 871–887.
[5] Jimenez, J.L., Guijarro, J.I., Orlova, E., Zurdo, J., Dobson, C.M., Sunde, M. and Saibil, H.R. (1999) Cryo-electron microscopy structure of an SH3 amyloid fibril and model of the molecular packing. EMBO J. 18, 815–821.
[6] Serpell, L.C., Sunde, M., Benson, M.D., Tennent, G.A., Pepys, M.B. and Fraser, P.E. (2000) The protofilament substructure of amyloid fibrils. J. Mol. Biol. 300, 1033–1039.
[7] Makin, O.S. and Serpell, L.C. (2002) Examining the structure of the mature amyloid fibril. Biochem. Soc. Trans. 30, 521–525.
[8] Serpell, L.S. (2000) Alzheimer's amyloid fibrils: structure and assembly. Biochim. Biophys. Acta 1502, 16–30.
[9] Guijarro, J.I., Sunde, M., Jones, J.A., Campbell, I.D. and Dobson, C.M. (1998) Amyloid fibril formation by an SH3 domain. Proc. Natl. Acad. Sci. USA 95, 4224–4228.
[10] Litvinovich, S.V., Brew, S.A., Aota, S., Akiyama, S.K., Haudenschild, C. and Ingham, K.C. (1998) Formation of amyloid like fibrils by self association of a partially unfolded fibronectin type III module. J. Mol. Biol. 280, 245–258.
[11] Chiti, F., Webster, P., Taddei, N., Clark, A., Stefani, M., Ramponi, G. and Dobson, C.M. (1999) Designing conditions for in vitro formation of amyloid protofilaments and fibrils. Proc. Natl. Acad. Sci. USA 96, 3590–3594.
[12] Fandrich, M., Fletcher, M.A. and Dobson, C.M. (2001) Amyloid fibrils from muscle myoglobin. Nature 410, 165–166.
[13] Sirangelo, I., Malmo, C., Casillo, M., Mezzogiorno, A., Papa, M. and Irace, G. (2002) Tryptophanyl substitution in apomyoglobin determine protein aggregation and amyloid-like fibril formation at physiological pH. J. Biol. Chem. 277, 45887–45891.
[14] Sirangelo, I., Malmo, C., Iannuzzi, C., Mezzogiorno, A., Bianco, M.R., Papa, M. and Irace, G. (2004) Fibrillogenesis and cytotoxic activity of the amyloid-forming apomyoglobin mutant W7FW14F. J. Biol. Chem. 279, 13183–13189.
[15] Bucciantini, M., Giannoni, E., Chiti, F., Baroni, F., Formigli, L., Zurdo, J., Taddei, N., Ramponi, G., Dobson, C.M. and Stefani, M. (2002) Inherent toxicity of aggregates implies a common mechanism for protein misfolding disease. Nature 416, 507–511.
[16] Dobson, C.M. (2001) The structural basis of protein folding and its links with human disease. Philos. Trans. R. Soc. Lond. B: Biol. Sci. 356, 133–145.
[17] Dobson, C.M. (2003) Protein folding and misfolding. Nature 426, 884–890.
[18] Fandrich, M. and Dobson, C.M. (2002) The behaviour of polyamino acids reveals an inverse side chain effect in amyloid structure formation. EMBO J. 21, 5682–5690.
[19] Chiti, F., Taddei, N., Baroni, F., Capanni, C., Stefani, M., Ramponi, G. and Dobson, C.M. (2002) Kinetics partitioning of protein folding and aggregation. Nat. Struct. Biol. 9, 137–143.
[20] Selkoe, D.J. (2001) Alzheimer's disease: genes, proteins, and therapy. Physiol. Rev. 81, 741–766.
[21] Goedert, M., Ghetti, B. and Spillantini, M.G. (2000) Tau genes mutations in frontotemporal dementia and Parkinsonism linked to chromosome 17 (FTDP-17). Their relevance for understanding the neurodegenerative process. Ann. NY Acad. Sci. 920, 74–83.
[22] Volles, M.J. and Lansbury Jr., P.T. (2002) Vesicle permeabilization by protofibrillar alpha-syneuclin is sensitive to Parkinson's disease-linked mutations and occurs by a pore-like mechanism. Biochemistry 41, 4595–4602.
[23] Rochet, J.C. and Lansbury Jr., P.T. (1998) Amyloid fibrillogenesis. Themes and variations. Curr. Opin. Struct. Biol. 8, 101–106.
[24] Chiti, F., Stefani, M., Taddei, N., Ramponi, G. and Dobson, C.M. (2003) Rationalizaton of the effects of mutations on peptide and protein aggregation rates. Nature 424, 805–808.
[25] Calamai, M., Taddei, N., Stefani, M., Ramponi, G. and Chiti, F. (2003) Relative influence of hydrophobicity and net charge in the aggregation of two homologous proteins. Biochemistry 42, 15078–15083.
[26] Fandrich, M., Forge, V., Buder, K., Kittler, M., Dobson, C.M. and Diekmann, S. (2003) Myoglobin forms amyloid fibrils by association of unfolded polypeptide segments. Proc. Natl. Acad. Sci. USA 100 (26), 15463–15468.
[27] Balestrieri, C., Colonna, G. and Irace, G. (1973) The skeletal muscle myoglobin of water buffalo (*Bos Bubalus* L.). Comp. Biochem. Physiol. 46B, 667–672.
[28] Teale, F.W.J. (1959) Cleavage of the heme protein by acid methylethylketone. Biochim. Biophys. Acta 35, 543.
[29] Wetlaufer, D.B. (1962) Ultraviolet spectra of proteins and amino acids. Adv. Protein Chem. 17, 303–390.
[30] Naiki, H., Higuchi, K., Hosowaka, M. and Takeda, T. (1989) Fluorometric determination of amyloid fibrils in vitro using the fluorescent dye, thioflavin T1. Anal. Biochem. 177, 244–249.
[31] Chow, C.C., Chow, C., Ragunathan, V., Huppert, T.J., Kimball, E.B. and Cavagnero, S. (2003) Chain length dependence of apomyoglobin folding: structural evolution from misfolded sheets to native helices. Biochemistry 42, 7090–7099.
[32] Waltho, J.P., Feher, V.A., Merutka, G., Dyson, H.J. and Wright, P.E. (1993) Secondary structure formation by peptides corresponding to the G- and H-helices of myoglobin. Biochemistry 32, 6337–6347.
[33] Dosi, R. (2005) Ph.D. Thesis, Caratterizzazione strutturale chimico-fisica e cinetica della mioglobina di bufalo (*Bubalus Bubalis*), Biblioteca Nazionale Centrale di Roma.